12th International Symposium on Turbulence and Shear Flow Phenomena (TSFP12)
Osaka, Japan (Online), July 19-22, 2022

# DEEP MEAN-FIELD MODELING OF TRANSIENT AND POST-TRANSIENT, MULTI-ATTRACTOR FLOW DYNAMICS – EXEMPLIFIED FOR THE FLUIDIC PINBALL

**Nan Deng**
School of Mechanical Engineering and Automation
Harbin Institute of Technology, Shenzhen
518055, People's Republic of China
dengnan@hit.edu.cn

**Luc R. Pastur**
Unité de Mécanique, IMSIA
ENSTA-Paris, Institut Polytechnique de Paris
F-91120 Palaiseau, France
luc.pastur@ensta-paris.fr

**Marek Morzyński**
Department of Virtual Engineering
Poznań University of Technology
PL 60-965 Poznań, Poland
morzynski@virtual.edu.pl

**Bernd R. Noack**
School of Mechanical Engineering and Automation
Harbin Institute of Technology, Shenzhen
518055, People's Republic of China
bernd.noack@hit.edu.cn

## ABSTRACT

We propose three kinds of mean-field modeling strategies for the complex dynamics generally found in fluid mechanics. A key enabler is a mean-field assumption, where slowly-varying mean-field deformations are due to the fluctuating field through the Reynolds stress, resulting in a Reynolds-like decomposition. We have developed projection-based and cluster-based reduced-order models, i.e., a least-order mean-field model for the successive bifurcations (Deng *et al.*, 2020), an aerodynamic force model associated with a Galerkin model (Deng *et al.*, 2021), and a hierarchical network model to automate the identification of multi-attractor dynamics (Deng *et al.*, 2022). These mean-field models are exemplified for a challenging test case of the fluidic pinball at $Re = 80$, characterized by six invariant sets (three steady solutions and three limit cycles) induced by the first two successive bifurcations of pitchfork and Hopf types. This work shows a paradigm for automatable reduced-order modeling of complex flows using first principles and machine learning techniques, balancing between data-driven and physics-driven approaches and improving model interpretability and generalizability.

## MODELING COMPLEX FLOW DYNAMICS

The complexity of the fluid flow comes from its high dimensionality, nonlinearity, and multiscale spatial and temporal behavior. A massive amount of flow detail information will be generated for increasing resolution when dealing with fluid flow problems. It is hard to understand all these details of different scales, and the control optimization is impossible to be applied. Reduced-order modeling aims to obtain simplified, interpretable models of complex systems. Discussing and analyzing the dynamics in this low-dimensional approximated system makes it possible to understand the underlying mechanisms and design the control laws. Such low-dimensional models are essential for flow dynamics prediction, effective control, and optimization (Rowley & Dawson, 2017).

In the era of big data, extracting physical laws of complex nonlinear phenomena and constructing parsimonious models from data is one of the frontier hotspots. Artificial Intelligence (AI) methods and Machine Learning (ML) techniques are revolutionizing our traditional paradigm of modeling and control in fluid mechanics (Brunton *et al.*, 2020). However, data-driven approaches cannot guarantee the models' stability, generalization, and physical interpretability. Combining first principles and a priori physical information into the modeling process is the key to promising solutions to this problem.

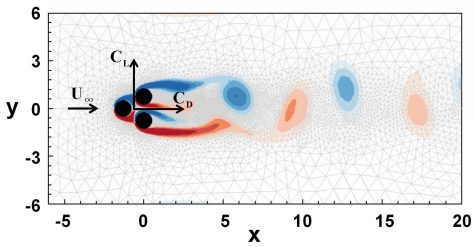


Figure 1. Flow configuration of the fluidic pinball. A vorticity field is color-coded in the range $[-1.5, 1.5]$ from blue to red. Drag and lift coefficients are denoted with $C_D$ and $C_L$.

In this presentation, we will start with the weakly nonlinear analysis under the mean-field consideration and develop three kinds of modeling strategies for the complex wake dynamics of the fluidic pinball. The resulting models are used to describe the transient and post-transient, multi-attractor dynamics of the successive bifurcations, the instantaneous aerodynamic force, and a multiscale topography of global and local dynamics .

### Fluidic pinball

As shown in Fig. 1, the fluidic pinball consists of three fixed cylinders, whose axes are placed on the vertices of an equilateral triangle in the $(x,y)$ plane and perpendicularly to this plane. The gap distance is one radius between every two

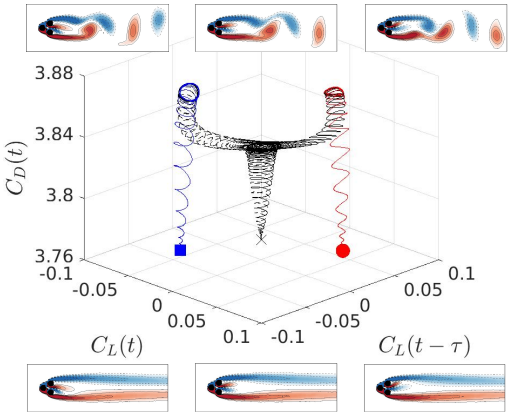


Figure 2. Trajectories in the time-delayed embedding space of the force coefficients (lift, lift with time delay and drag) from the three unstable steady solutions (bottom) to the three periodic solutions at $Re = 80$. A snapshot is taken for each periodic solution and shown on the top.

cylinders. The upstream flow $U_\infty$ is uniform in the streamwise direction $\mathbf{e}_x$ at the inlet.

The transient and post-transient dynamics at different Reynolds numbers are numerically investigated by Direct Numerical Simulation (DNS). At $Re = 80$, three steady solutions and three periodic solutions (limit cycles) can be found due to two successive instabilities, as shown in Fig. 2, henceforth providing a challenging test case for the derivation of a predictive force model. We consider multiple trajectories starting from the vicinity of the three steady solutions. More details for quasi-periodic and chaotic dynamics at higher Reynolds numbers can be found in Deng *et al.* (2020).

## MEAN-FIELD ANSATZ

Under the mean-field consideration, the triple decomposition of the flow field reads

$$\mathbf{u}(\mathbf{x},t) = \underbrace{\langle \mathbf{u}(\mathbf{x},t)\rangle_T}_{\omega \ll \omega_c} + \underbrace{\tilde{\mathbf{u}}(\mathbf{x},t)}_{\omega \sim \omega_c} + \underbrace{\mathbf{u}'(\mathbf{x},t)}_{\omega \gg \omega_c}, \tag{1}$$

where the dominant angular frequency $\omega_c$ is defined as the dominant peak in the Fourier spectrum of the velocity field. The velocity field is decomposed into a slowly-varying mean-flow field $\langle \mathbf{u}\rangle_T$, a coherent component on timescales of order $2\pi/\omega_c$, involving coherent structures $\tilde{\mathbf{u}}$, and a remaining (supposedly) non-coherent small scale fluctuations $\mathbf{u}'$. This kind of decomposition follows the weakly nonlinear analysis in building the low-order Galerkin models of Tadmor *et al.* (2011).

From the mean-field theory, the slowly-varying mean-flow field evolves out of the steady solution under the action of the Reynolds stress associated with the most unstable eigenmode(s). The mean-flow field deformation $\mathbf{u}_\Delta$ is used to describe the difference between the slowly-varying mean flow and the invariant base flow $\mathbf{u}_s(\mathbf{x})$, which reads

$$\langle \mathbf{u}(\mathbf{x},t)\rangle_T = \mathbf{u}_s(\mathbf{x}) + \mathbf{u}_\Delta(\mathbf{x},t). \tag{2}$$

The linear dynamics only involve a minimal neighborhood of the base flow $\mathbf{u}_s$, as the perturbation is tiny at the onset of the instability. As the perturbation develops, the nonlinear term cannot be ignored and will start to modify the base flow. Hence, the mean flow deformation comes from the effect of the Reynolds stresses of the coherent component $\overline{(\tilde{\mathbf{u}}\cdot\nabla)\tilde{\mathbf{u}}}$ and of the non-coherent small scale fluctuations $\overline{(\mathbf{u}'\cdot\nabla)\mathbf{u}'}$. During the mean-field distortion from the base flow $\mathbf{u}_s$ to the mean flow, the original linear dynamics is no longer valid, and the nonlinear interactions will drive the transient dynamics until saturation. For the transient and post-transient dynamics, the slaving relation between the active modes (fluctuations) and the shift modes (mean-field distortion) and their timescale difference can be used to improve model interpretability in a data-driven modeling process.

## MEAN-FIELD MODELS

In this section, we briefly introduce the three kinds of mean-field modeling methodologies and discuss their results.

### Least-order mean-field model

For the Galerkin framework, the velocity field $\mathbf{u}(\mathbf{x},t)$ is decomposed in a basic mode $\mathbf{u}_0(\mathbf{x})$ with amplitude $a_0 \equiv 1$ and a fluctuating contribution

$$\mathbf{u}(\mathbf{x},t) = \sum_{i=0}^{N} a_i(t)\mathbf{u}_i(\mathbf{x}), \tag{3}$$

where the fluctuation is represented by a Galerkin approximation of $N$ orthonormal space-dependent modes $\mathbf{u}_i(\mathbf{x})$, $i = 1,\ldots,N$, with time-dependent amplitudes $a_i(t)$.

The Galerkin expansion in Eq.(3) satisfies the incompressibility condition and the boundary conditions by construction. The evolution equation for the mode amplitudes $a_i$ is derived by a Galerkin projection of the Navier-Stokes equations onto the modes $\mathbf{u}_i$:

$$\frac{d}{dt}a_i = \nu \sum_{j=0}^{N} l_{ij}^{\nu} a_j + \sum_{j,k=0}^{N} q_{ijk}^{c} a_j a_k + \sum_{j,k=0}^{N} q_{ijk}^{p} a_j a_k, \tag{4}$$

with the coefficients $l_{ij}^{\nu} = \left(\mathbf{u}_i, \triangle \mathbf{u}_j\right)_\Omega$, $q_{ijk}^{c} = \left(\mathbf{u}_i, \nabla\cdot \mathbf{u}_j \otimes \mathbf{u}_k\right)_\Omega$ and $q_{ijk}^{p} = \left(\mathbf{u}_i, -\nabla p_{jk}\right)_\Omega$ for the viscous, convective and pressure terms in the Navier-Stokes equations, respectively.

The Galerkin system, as in Eq.(4), directly derived from the Galerkin projection of the leading Proper Orthogonal Decomposition (POD) modes, cannot capture the transient and post-transient dynamics correctly. It introduces extremely long transients due to the underestimated growth rate. In a least-order mean-field model, we represent the flow dynamics with the fewest number of degrees of freedom, as shown in Fig. 3(left). The basic modes are chosen with the knowledge of the instabilities that the system has undergone while increasing the Reynolds number. Based on an optimal low-dimensional basis, a general Galerkin framework leads to the linear-quadratic Ordinary Differential Equations (ODE) with normal forms of the corresponding bifurcations, as shown in Fig. 3(right). We allow the cross-terms to exist for the coupling relationship between the degrees of freedom of two bifurcations. Our strategy is to correct some of the system coefficients by the knowledge provided by the linear stability analysis and the asymptotic dynamics. The remaining coefficients of the nonlinear interaction terms are identified by a sparse regression algorithm with physics-based constraints, namely the

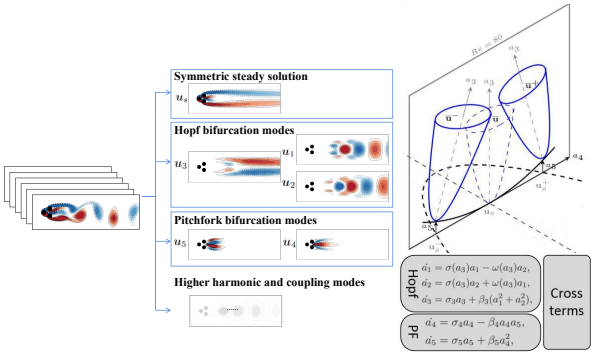


Figure 3. Least-order mean-field model at $Re = 80$, with the elementary degrees of freedom based on bifurcations (left) and the dynamical system with normal forms of corresponding bifurcations. See Deng *et al.* (2020) for the details.

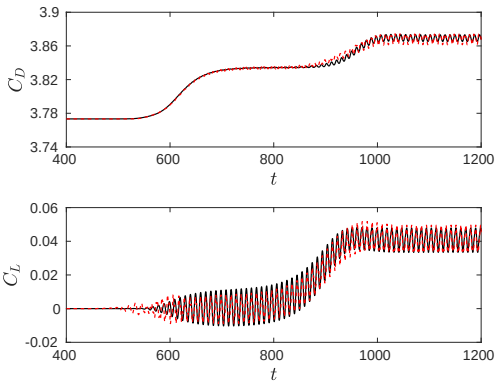


Figure 4. Time evolution of the drag and lift coefficients in the full-flow dynamics (solid black) and for the force model (red dashed), at $Re = 80$.

constrained sparse Galerkin regression (Brunton *et al.*, 2016; Loiseau & Brunton, 2018). The least-order model is only five-dimensional but can reproduce the key features of the full dynamics (Deng *et al.*, 2020).

## Galerkin force model

Force computations on immersed bodies are of particular concern in engineering fluid mechanics. Despite the wide use of POD-Galerkin for reduced-order modeling in industry, systematic investigations and interpretations of the aerodynamic force in the Galerkin framework are mostly missing. Previous studies of Noca *et al.* (1999) revealed that the force on an immersed body can be expressed simply in terms of the velocity field and its derivatives. Based on this idea, Liang & Dong (2014) derived a force expression with the forces of each velocity-based POD mode and the forces from the interaction between the POD modes. The Galerkin force model proposed in our study reveals that the force on the body is a constant-linear-quadratic function of the mode amplitudes from a Galerkin expansion. In addition, physical constraints and sparse calibration can be further used to improve the human interpretability of the resulting models.

Based on the Galerkin expansion of Eq.(3), the instantaneous force on the body can be derived as a function of the mode amplitudes from first principles. Let $\Gamma$ be the boundary of the body in the flow domain $\Omega$ and $\mathbf{n}$ the unit normal pointing outward from the surface element $dS$. The viscous force component in direction $\mathbf{e}_\alpha$ of the velocity mode $\mathbf{u}_j$ is expressed as

$$q^{\nu}_{\alpha;j} = 2\nu \oint_\Gamma \sum_{\beta=x,y} S_{\alpha,\beta}(\mathbf{u}_j)\, n_\beta \, dS, \tag{5}$$

where the strain rate tensor $S_{\alpha,\beta} = \left(\partial_\alpha u_\beta + \partial_\beta u_\alpha\right)/2$ with indices $\alpha,\beta = x,y$. The pressure force involves two velocity modes from the pressure Poisson equation

$$\nabla^2 p_{jk} = \nabla\cdot\left(-\nabla\cdot\mathbf{u}_j\otimes\mathbf{u}_k\right) = -\sum_{\alpha=x,y}\sum_{\beta=x,y} \partial_\alpha u_\beta(\mathbf{u}_j)\,\partial_\beta u_\alpha(\mathbf{u}_k), \tag{6}$$

and the force component in $\alpha$-direction is expressed as

$$q^{p}_{\alpha;jk} = -\oint_\Gamma dS\, n_\alpha p_{jk}. \tag{7}$$

Hence, the total force can be expressed as a constant-linear-quadratic expression in terms of the mode coefficients

$$F_\alpha = F^{\nu}_\alpha + F^{p}_\alpha = \sum_{j=0}^{N} l^{\nu}_{\alpha;j} a_j + \sum_{j,k=0}^{N} q^{p}_{\alpha;jk} a_j a_k. \tag{8}$$

As $a_0 \equiv 1$, the drag (in direction $\mathbf{e}_x$) and lift (in direction $\mathbf{e}_y$) coefficients can be derived as a constant-linear-quadratic expression in terms of the mode coefficients,

$$C_D = c_x + \sum_{j=1}^{N} l_{x;j} a_j + \sum_{j,k=1}^{N} q_{x;jk} a_j a_k, \tag{9}$$

$$C_L = c_y + \sum_{j=1}^{N} l_{y;j} a_j + \sum_{j,k=1}^{N} q_{y;jk} a_j a_k, \tag{10}$$

where $c_\alpha = q^{\nu}_{\alpha;0} + q^{p}_{\alpha;00}$, $l_{\alpha;j} = q^{\nu}_{\alpha;j} + q^{p}_{\alpha;j0} + q^{p}_{\alpha;0j}$, and $q_{\alpha;jk} = q^{p}_{\alpha;jk}$.

The drag and lift formulae are simplified for the fluidic pinball exploiting the symmetry of the modes. Approximately half of the terms can be discarded on the grounds of symmetry. A second simplification is performed with a sparse calibration of the remaining coefficients. We employ the constrained SINDy (sparse identification of nonlinear dynamics) algorithm (Brunton *et al.*, 2016; Loiseau & Brunton, 2018), and the sparsity parameter $\lambda$ penalizes any non-vanishing term and yields sparse human-interpretable expressions.

The resulting drag and lift formulae show long-term agreement with the force coefficients in the full-flow dynamics from DNS, based on a mean-field Galerkin model with only seven degrees of freedom, as shown in Fig. 4. The sparse force model successfully describes multi-attractor behaviour even for the complex dynamics with six exact solutions. We provide a detailed discussion on the challenges of applying the purely projection-based approach and using standard POD modes in Deng *et al.* (2021).

In summary, we proposed an aerodynamic force formulae complementing mean-field POD-Galerkin models for the unforced fluidic pinball. We envision successful applications of sparse regression for aerodynamic forces for turbulent flows. The force formula may be particularly instructive for drag reduction with active control. Given a Galerkin model, the force formula indicates beneficial regions of the state space. Thus, an upfront kinematical insight is gained in which direction control needs to 'push' the attractor.

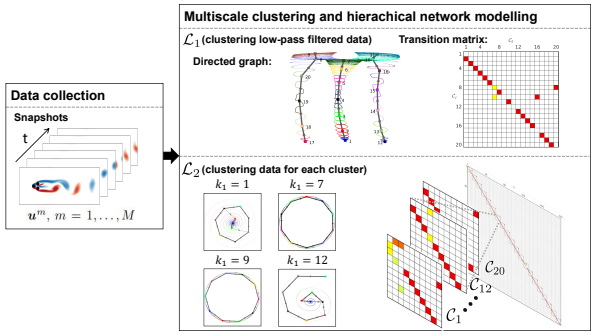


Figure 5. Sketch for HiCNM applied to the fluidic pinball at $Re = 80$, see Deng *et al.* (2022) for details.

## Hierachical cluster-based network model

Automated reduced-order modeling is one of the most challenging and exciting directions for complex nonlinear dynamics. The traditional modeling techniques, like Galerkin modeling, always project the original system onto a low-dimensional subspace and model an approximate dynamical system with an optimal basis (Taira *et al.*, 2017). The projection basis decides the closeness of the approximate dynamics to the full dynamics. Data-driven modeling can liberate us from the issue of choosing the projection basis and provide us with novel and promising modeling strategies from mathematics, data science, and statistical physics. In this subsection, we briefly overview the hierarchical modeling strategy, which presents great consistency with the Reynolds decomposition and shows its great potential for multi-scale and multi-frequency modeling.

Modal analysis-based modeling relies on the designer's empirical and theoretical knowledge to select modes and construct subspace. In contrast, Cluster-based ROM (CROM) or Network Model (CNM) can effectively avoid these challenges (Kaiser *et al.*, 2014; Fernex *et al.*, 2021). The clustering algorithm achieves a kinematic compression of the input data $\mathbf{u}^m$, $m = 1,\dots,M$, by grouping the similar states into the clusters $\mathscr{C}_k$, $k = 1,\dots,K$. The snapshots are featured by statistical averages of the grouping data (centroids) in the original data space by $k$-means algorithm and are labeled with a cluster index $k^m = k$, $k = 1,\dots,K$. As in the state space without approximation, the identified manifold can preserve the original structure depending on the cluster distribution. The CROMs are expected to replace the traditional modeling methods as a more generic means of modeling flow dynamics.

According to the minimization strategy of $k$-means algorithm, the clustering is optimal for the spatial distributions of the centroids but not for the dynamics. The classical CROM may face difficulties with multi-scale problems in transient and post-transient dynamics because the clustering results are highly dependent on the spatial distances in the state space. The critical enabler for applying CNM to the transient and post-transient dynamics is the triple decomposition under the mean-field consideration, as in Eq.(1). By decomposing the flow into a hierarchy of components, we can systematically model the dynamics at different scales, as shown in Fig. 5.

A self-supervised hierarchical clustering is performed from top to bottom, which prioritizes the modeling of global trends for the mean flow distortion, then refines the local dynamics with sub-clusters. Both the global trends and the local structure during the transition can be well preserved by a fewer number of clusters in the hierarchical structure, which leads to a better understanding of the physical mechanisms involved in the flow dynamics.

In summary, the Hierarchical Cluster-based Network Model (HiCNM) introduces hierarchical structure into the CNM from the mean-field considerations, which enables systematically identifying the transient and post-transient dynamics between multiple invariant sets in a self-supervised manner and steps towards automated ROM of complex dynamics. HiCROM inherits the excellent recognition performance of CROM and provides a generalized modeling strategy for complex dynamics with multiple scales and frequencies.

## CONCLUSIONS

We propose combining the mean-field assumption in fluid flow and data-driven ML methods to optimize the ROM methods for complex flow dynamics. In the classic POD-Galerkin framework, the mean-field assumption leads to a least-order constrained Galerkin system, where the degrees of freedom are optimal with respect to the underlying instabilities in the system. Based on the Galerkin expansion, the instantaneous force on the body is derived as a constant-linear-quadratic function of the mode amplitudes from first principles. The force model can be further simplified using symmetry properties and sparse calibration. The HiCROM can systematically identify the multi-scale dynamics, including the transitions between different Navier-Stokes solutions, the bifurcating dynamics into different attractors, and the local structures from destabilization to saturation stages. All the above-mentioned modeling strategies are exemplified for the transient and post-transient dynamics of the unforced fluidic pinball at $Re = 80$ and result in low-dimensional, sparse, human-interpretable mean-field models.

This will be a fruitful area for advancing automated ROM with first-principles and AI methods for complex dynamical systems in flow mechanics and industrial applications (like vehicles, trains, airplanes, and other nonlinear dynamics) to achieve a deeper understanding of physical mechanisms, dynamics estimation, state control, and optimization.

## REFERENCES

Brunton, S. L., Noack, B. R. & Koumoutsakos, P. 2020 Machine learning for fluid mechanics. *Ann. Rev. Fluid Mech.* **52** (1), 477–508.

Brunton, S. L., Proctor, J. L. & Kutz, J. N. 2016 Discovering governing equations from data by sparse identification of nonlinear dynamical systems. *Proc. Natl. Acad. Sci.* **113** (5), 3932–3937.

Deng, N., Noack, B. R., Morzyński, M. & Pastur, L. R. 2020 Low-order model for successive bifurcations of the fluidic pinball. *J. Fluid Mech.* **884**, A37.

Deng, N., Noack, B. R., Morzyński, M. & Pastur, L. R. 2021 Galerkin force model for transient and post-transient dynamics of the fluidic pinball. *J. Fluid Mech.* **918**, A4.

Deng, N., Noack, B. R., Morzyński, M. & Pastur, L. R. 2022 Cluster-based hierarchical network model of the fluidic pinball – cartographing transient and post-transient, multi-frequency, multi-attractor behaviour. *J. Fluid Mech.* **934**, A24.

Fernex, Daniel, Noack, Bernd R & Semaan, Richard 2021 Cluster-based network modeling—from snapshots to complex dynamical systems. *Science Advances* **7** (25), eabf5006.

Kaiser, E., Noack, B. R., Cordier, L., Spohn, A., Segond, M., Abel, M., Daviller, G., Östh, J., Krajnović, S. & Niven, R. 2014 Cluster-based reduced-order modelling of a mixing layer. *J. Fluid Mech.* **754**, 365–414.

Liang, Z. & Dong, H. 2014 Virtual force measurement of POD modes for a flat plate in low reynolds number flows. *AIAA Paper* pp. 2014–0054.

Loiseau, J. C. & Brunton, S. L. 2018 Constrained sparse galerkin regression. *J. Fluid Mech.* **838**, 42—-67.

Noca, F., Shiels, D. & Jeon, D. 1999 A comparison of methods for evaluating time-dependent fluid dynamic forces on bodies, using only velocity fields and their derivatives. *J. Fluids Struct.* **13** (5), 551–578.

Rowley, C. W. & Dawson, S. T. 2017 Model reduction for flow analysis and control. *Ann. Rev. Fluid Mech.* **49**, 387–417.

Tadmor, G., Lehmann, O., Noack, B. R., Cordier, L., Delville, J., Bonnet, J.-P. & Morzyński, M. 2011 Reduced order models for closed-loop wake control. *Philos. Trans. R. S. A* **369** (1940), 1513–1524.

Taira, Kunihiko, Brunton, Steven L, Dawson, Scott TM, Rowley, Clarence W, Colonius, Tim, McKeon, Beverley J, Schmidt, Oliver T, Gordeyev, Stanislav, Theofilis, Vassilios & Ukeiley, Lawrence S 2017 Modal analysis of fluid flows: An overview. *AIAA Journal* **55** (12), 4013–4041.